Supplementary Material

Emission Characteristics of VOCs from On-road Vehicles in an Urban Tunnel in Eastern China and Prediction for 2017–2026

Chengxun Deng[1], Yujuan Jin[1], Min Zhang[2*], Xiaowei Liu[3], Zhimin Yu[1*]

[1]Department of Biological and Environmental Engineering, Hefei University, Hefei City, 230022, China

[2]Anhui Environmental Monitoring Center Station, Hefei City, 230071, China

[3]School of Resources and Environmental Engineering, Hefei University of Technology, Hefei City, 230009, China

[*] Corresponding author. Tel: 0-86-0551-62158447

E-*mail address*: yuzhimin@hfuu.edu.cn

1. Determination of the optimal sampling points in the tunnel

The tunnel spatial distribution and time distribution experiments were used to understand the distribution characteristics of pollutants in the tunnel over time and across space, thus allowing the appropriate distribution of the sampling points for the tunnel experiment and improving the accuracy for the estimation of VOC emission factors. Nine types of VOCs (2-methylbutane, n-pentane, n-hexane, benzene, toluene, ethylbenzene, m/p-xylene, o-xylene, and styrene) with a high detection rate in the two experiments were selected as the study objects to analyze the distribution of VOCs from vehicles in the tunnel.

Samples were collected once in the early morning, late morning, and late afternoon, and the sampling periods were 4:30–5:30, 9:30–10:30, and 17:30–18:30, respectively, and 1-h sampling was performed at each sampling period. In the tunnel, five sampling points were uniformly distributed through the tunnel as follows: 200 m from the entrance of the tunnel (#1), 450 m from the entrance of the tunnel (#2), the middle of the tunnel (#3), 950 m from the exit of the tunnel (#4), and 1235 m from the exit of the tunnel (#5). Background points were set outside the tunnel to monitor the background concentration of VOCs in the atmosphere and eliminate the contribution of other man-made sources of pollution. The results of preliminary spatial distribution experiments showed that the total amount of VOCs decreased slightly from point #1 to point #2, increased gradually to the peak from point 2 to point 3, decreased gradually from point #3 to point #5 (Fig. S1 and Fig. S2). The high concentration at the middle sampling point #3 was mainly because the tunnel was relatively long and the presence of air inflow at the exit of the tunnel caused the concentration at the exit to be lower than that at the middle point where the diffusion capacity was weak.

2. Determination of sampling time

Two sampling points were set at a distance of 825 m (point #6) from the entrance and at a distance of 450 m from the exit of the tunnel (point #4), and background points were set outside the tunnel. The sampling period was between 6:00 and 21:00. Instantaneous sampling was performed every 2 h but the sampling frequency was increased to once per hour during the peak traffic period, and the specific time intervals were as follows: 6:00, 8:00, 9:00, 10:00, 12:00, 13:00, 14:00, 16:00, 18:00, 19:00, 20:00, and 21:00.

3. Calculation of vehicle population in Hefei in the next 10 years

3.1 Model calculation

According to the GM (1, 1) forecasting principle, a prediction model for the vehicle population in Hefei was established, and the parameters of the model were calculated using Hefei 2012–2016 vehicle population data. The vehicle population data sequence for 2012–2016 was $x^{(0)}$ = (97.61, 104.54, 121.63, 138.86, 158.48), the new generated sequences were accumulated, and the randomness of the original data sequence was mitigated: $x^{(1)}$ = (97.61, 202.15, 323.78, 462.64, 621.12).

First-order linear albinism differential equation related to $x^{(1)}(k)$ was established $\frac{dx^{(1)}}{dt} + ax^{(1)} = \beta$. The least square method was used to solve the grey parameters α and β, i.e., $\mathbf{A} = \begin{pmatrix} \alpha \\ \beta \end{pmatrix} = (B^T B)^{-1}(B^T Y_n)$, and the matrix B and vector Y_n were as follows:

$$B = \begin{pmatrix} -0.5(x^{(1)}(1) + x^{(1)}(2)) & 1 \\ -0.5(x^{(1)}(2) + x^{(1)}(3)) & 1 \\ . & . \\ . & . \\ . & . \\ -0.5(x^{(1)}(n-1) + x^{(1)}(n)) & 1 \end{pmatrix} = \begin{pmatrix} -149.88 & 1 \\ -262.97 & 1 \\ -393.21 & 1 \\ -541.88 & 1 \end{pmatrix}, \quad Y_n = \begin{pmatrix} x^{(0)}(1) \\ x^{(0)}(2) \\ . \\ . \\ . \\ x^{(0)}(n) \end{pmatrix}$$

According to the equation, B^TB, $(B^TB)^{-1}$, B^TY_n and A were obtained.

$$B^T B = \begin{pmatrix} 271347.2498 & -964.54 \\ -964.54 & 4 \end{pmatrix} \qquad (B^T B)^{-1} = \begin{pmatrix} 2.58\times10^{-5} & 6.22\times10^{-3} \\ 6.22\times10^{-3} & 1.75 \end{pmatrix}$$

$$B^T Y_n = \begin{pmatrix} -127370.54 \\ 523.51 \end{pmatrix} \qquad (B^T B)^{-1} B^T Y_n = \begin{pmatrix} -0.0293 \\ 123.8234 \end{pmatrix}$$

Parameters α and β were calculated to be −0.0293 and 123.8, respectively.

3.2 Model validation

3.2.1. Residual test

By calculating the relative error between the original sequence and the grey prediction sequence, the model was judged by the magnitude of the residual.

(1) Calculation of residuals: $\Delta^{(0)}(k) = \mathrm{x}^{(0)}(k) - \hat{\mathrm{x}}^{(0)}(k) = \{0, -24.01, -10.74, 2.54, 18.11\}$.

(2) Calculation of relative error:

$$\varepsilon(k) = \frac{\mathrm{x}^{(0)}(k) - \hat{\mathrm{x}}^{(0)}(k)}{\mathrm{x}^{(0)}(k)} \times 100\% = \{0, -0.2297, -0.0883, 0.01829, 0.1143\}.$$

(3) Calculation of average residual: $\bar{\varepsilon} = \frac{1}{\mathrm{n\text{-}1}} \sum_{k=2}^{n} |\varepsilon(k)| = 11.26\%$.

(4) Calculation of model accuracy: $P^0 = 1 - \bar{\varepsilon} = 88.74\%$.

The above calculations showed that $\bar{\varepsilon} = 1.26\% < 20\%$, $P^0 = 88.74\% > 80\%$, and the model met the general requirements.

3.2.2. Stepwise ratio deviation test

(1) Calculation of the stepwise ratio of the model:

$$\delta^{(0)} = \frac{\hat{\mathrm{x}}^{(0)}(k\text{-}1)}{\hat{\mathrm{x}}^{(0)}(k)} = \{0.7593, 0.9711, 0.9710, 0.9711\}.$$

(2) Calculation of the stepwise ratio of the sequence:

$\sigma^{(0)}(k)=\frac{\mathrm{x}^{(0)}(k\text{-}1)}{\mathrm{x}^{(0)}(k)}=\{0.9337,0.8595,0.8759,0.8762\}$.

(3) Calculation of the stepwise ratio deviation:

$\rho(k)=\frac{\delta^{(0)}-\delta^{(0)}(k)}{\delta^{(0)}}\times 100\%=\{\text{-}47.04\%,11.49\%,9.79\%,9.77\%\}$. The absolute value of the deviation ratio deviation: $|\rho(k)|=\{47.04\%,11.49\%,9.79\%,9.77\%\}$.

(4) Average $\overline{\rho}$ of the absolute value of the stepwise ratio deviation:

$\overline{\rho}=\frac{1}{n-1}\sum_{k=2}^{n}|\rho(k)|=0.077$.

The above calculations showed that $\overline{\rho}$ =0.077 < 0.1, indicating higher requirements were met.

3.3.3. Degree of correlation test

(1) Calculation of the correlation coefficient:

$$\eta(k)=\frac{\min|\Delta^{(0)}(k)|+\rho\max|\Delta^{(0)}(k)|}{|\Delta^{(0)}(k)|+\rho\max|\Delta^{(0)}(k)|}=\{1,0.3333,0.5278,0.8254,0.3986\}$$

(2) Calculation of the degree of correlation: $r=\frac{1}{n}\sum_{k=1}^{n}\eta(k)=0.6170$

The calculation showed that the prediction accuracy of the model was satisfactory when r = 0.6170 ≥ 0.6.

3.3.4. Posterior variance test

(1) Calculation of the residuals and the average residual:

$\Delta^{(0)}(k)=|\mathrm{x}^{(0)}(k)-\hat{\mathrm{x}}^{(0)}(k)|=\{0,\text{-}24.01,\text{-}10.74,2.54,18.11\}$, and the average residual was −2.82.

(2) If the standard deviations of the original sequence $x^{(0)}$ and residual series Δ were S1andS2, respectively, then

$$S_1 = \sqrt{\frac{\sum\left[\mathrm{x}^{(0)}(k) - \overline{\mathrm{x}}^{(0)}\right]^2}{n-1}} = 24.951 \qquad S_2 = \sqrt{\frac{\sum\left[\Delta^{(0)}(k) - \overline{\Delta}^{(0)}\right]^2}{n-1}} = 1.7961$$

(3) Calculation of the posterior variance ratio: $C = \frac{S_2}{S_1} = 0.07198$

(4) Calculation of the small error probability: $P = P\left\{\left| \Delta^{(0)}(k) - \overline{\Delta}^{(0)} \right|\right\} < 0.6745 S_1 = 0.8$

The above calculations showed that $C = 0.07198$ and $P = 0.8$.

Table Captions

Table S1. Meteorological parameters of sampling points and periods in full experiment.

Table S2. Population of various types of vehicles

Table S3. Identification and quantification parameters for VOCs.

Table S4. 67 VOCs detected in the vehicle exhaust of Longchuang tunnel.

Table S1. Meteorological parameters of sampling points and periods in full experiment.

Sampling time	Sampling method	Temp. (°C)	Humidity	Wind speed (m/s)	light-duty vehicles (veh)	heavy-duty vehicles (veh)
6:00-7:00	One-hour sampling	24	78%	1.1 1.2 1.2 1.1	351	27
8:00-9:00	One-hour sampling	25	74%	2.2 2.4 2.6 2.1	933	27
9:00-10:00	One-hour sampling	26	71%	2.8 2.9 2.8 3.1	675	17
16:00-17:00	One-hour sampling	33	53%	1.7 2.1 1.9 1.7	639	69
18:00-19:00	One-hour sampling	32	49%	2.7 2.9 2.7 2.1	1071	48
19:00-20:00	One-hour sampling	31	51%	2.3 2.1 2.3 2.1	603	20
20:00-21:00	One-hour sampling	29	59%	1.9 2.1 2.3 1.7	408	18

Table S2. Population of various types of vehicles

	light-duty vehicles (veh)				heavy-duty vehicles (veh)	
	private cars	taxis	light trucks	mini buses	heavy-duty trucks	coach buses
6:00-7:00	211	80	29	31	17	10
8:00-9:00	510	261	60	102	11	16
9:00-10:00	321	235	45	74	7	10
16:00-17:00	373	167	50	49	30	39
18:00-19:00	653	305	48	65	21	27
19:00-20:00	312	189	44	58	16	4
20:00-21:00	207	120	49	32	16	2

Table S3. Identification and quantification parameters for VOCs.

Instruments	Model	Parameters
GC-MS	Agilent 7890A GC-597C MS	GC: the injector temperature was 140°C and the injection volume was 1 mL; the column temperature was initially set at 35°C kept for 5.0 min, then increased up to 150°C at a rate of 5°C/min (held for 7.0 min) and was maintained at 200°C for 4 min. Solvent delay time：5.6 min; helium carrier gas: 1.0 ml/min. MS: interface temperature: 250°C; scanning mode: SIM mode (230°C) with m/z ranges from 35 amu–300 amu; ionization method: EI (70ev).
Capillary column		60 m×0.25 mm, 1.4 μm film（6% Nitrile propyl phenyl -94% dimethyl polysiloxane stationary liquid）
Cryogenic-trap preconcentrator	Entech 7200	Sampling volume: 400 ml. First trap: capture temperature: -150°C; capture flow rate: 100 ml/min; desorption temperature: 10°C; valve temperature: 100°C; oven temperature: 150°C; oven time: 15 min. Secondary trap: capture temperature: -15°C; capture flow rate: 10 ml/min; capture time: 5 min; desorption temperature: 180°C; desorption time: 3.5 min; oven temperature: 190°C; oven time: 15 min. Third cryo-focus: focused time: -160°C; desorption time: 2.5 min; oven temperature: 200°C; oven time: 5 min. Transmission line temperature: 120°C.

Auto-sampler	ENTECH 7016D	/
Canister cleaning systems	ENTECH 3100D	/
Gas dilutor	ENTECH 4700	/
Sampling canister		Volume: 6L; pressure-withstanding value > 241 kPa.

Table S4. 67 VOCs detected in the vehicle exhaust of Longchuang tunnel.

Groups	Compounds	Groups	Compounds
Alkane	iso-butane		1,2-diethylbenzene
	n-butane	Halohydro-carbon	trichlorofluoromethane
	n-pentane		trichlorotrifluoroethane
	n-hexane		chloromethane
	n-heptane		dichloromethane
	octane		trichloromethane
	dodecane		carbon tetrachloride
	2-methylbutane		dichloroethane
	methylcyclopentane		1,2- propylene dichloride
	methylcyclohexane		1,3- propylene dichloride
	2,2-dimethylbutan	Alkene	2- butene
	cyclopentane		1- butene
	cyclohexane		trans-1-butene
	2-methylhexane		propylene
	3-methylpentane		2- pentene
	3-methylhexane		Trans-2-pentene
	2,2,3,3-tetramethylbutane		2-methyl-1-butene
	2-methyl heptane		2-methyl-1-pentene
	4-methyl heptane		4- methyl pentene
	ethylcyclohexane	OVOCs	1,2-dichloroethylene
Aromatics	benzene		1, 3-dichloroethylene
	methylbenzene		chloroethylene
	ethylbenzene		tetrachloroethylene
	propyl benzene		trichloro-ethylene
	cumene		styrene
	paraxylene		cyclopropyl-carbinol
	o-xylene		ethyl alcohol
	1,2,3-trimethylbenzene		acetaldehyde
	1,2,4- trimethylbenzene		dimethyl ether
	1,3,5- trimethylbenzene		acetone

1-ethyl-3-methylbenzene	2-butanone
1-ethyl-2-methylbenzene	ethyl acetate
1-ethyl-4-methylbenzene	sec-butyl acetate
1,4-diethylbenzene	

Figure Captions

Fig. S1. Concentrations of total VOCs at each sampling point.

Fig. S2. Concentrations of several typical VOCs at each sampling point.

Fig. S3. Comparison of the total VOCs (TVOCs) with the traffic flow at point #6.

Fig. S4. Comparison of the total VOCs (TVOCs) with the traffic flow at point #4.

Fig. S5. Composition of alkanes from vehicle exhausts in Longchuan Tunnel.

Fig. S6. Composition of aromatics (benzenes) from vehicle exhausts in Longchuan Tunnel.

Fig. S7. Composition of alkenes from vehicle exhausts in Longchuan Tunnel.

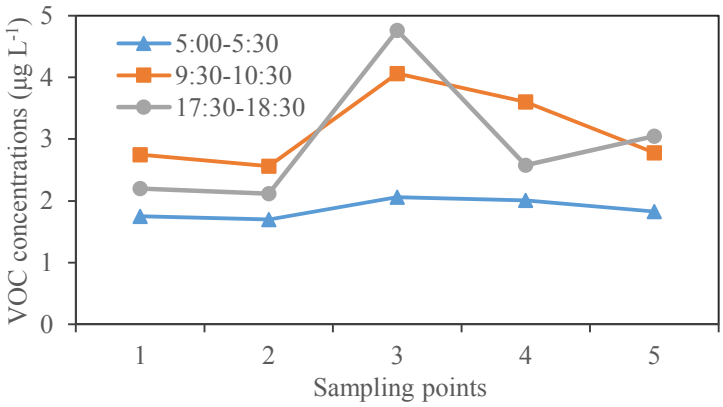

Fig. S1. Concentrations of total VOCs at each sampling point.

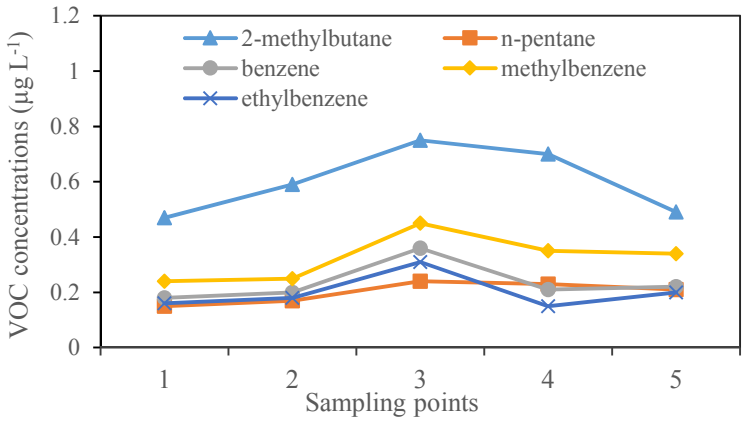

Fig. S2. Concentrations of several typical VOCs at each sampling point.

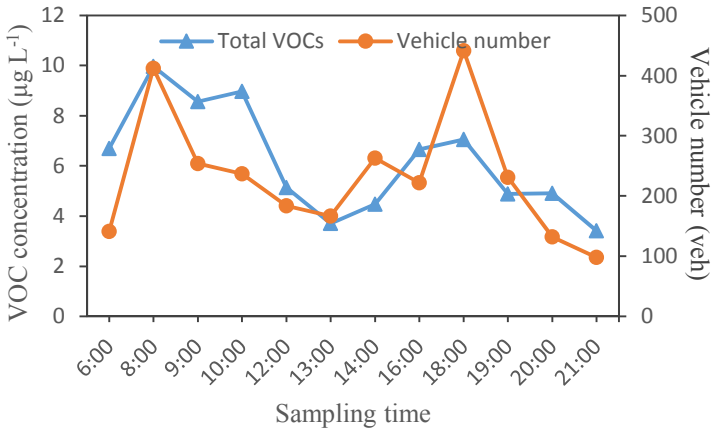

Fig. S3. Comparison of the total VOCs (TVOCs) with the traffic flow at point #6.

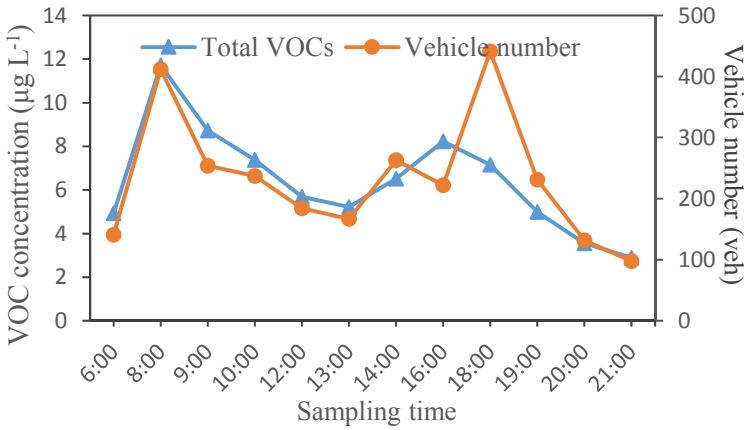

Fig. S4. Comparison of the total VOCs (TVOCs) with the traffic flow at point #4.

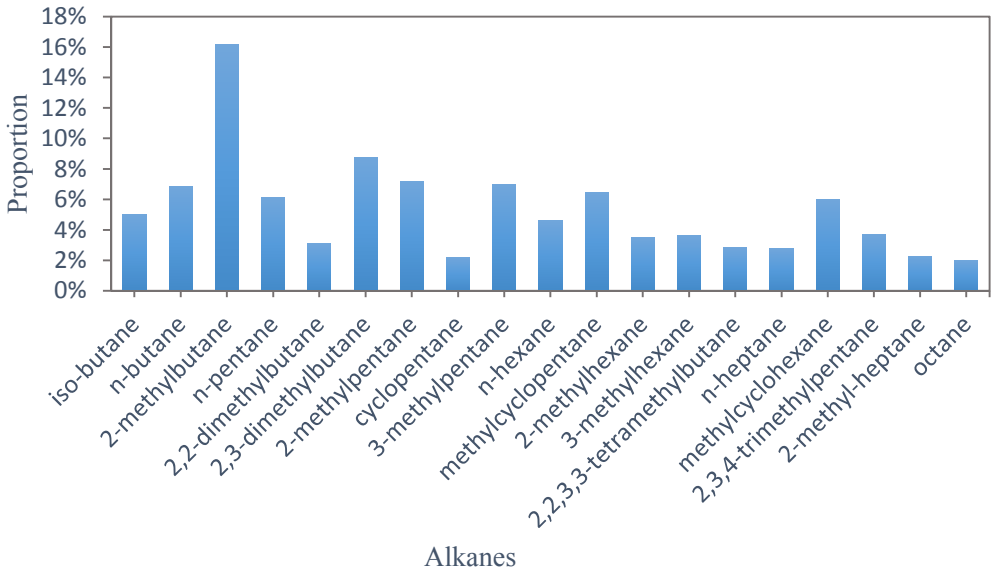

Fig. S5. Composition of alkanes from vehicle exhausts in Longchuan Tunnel.

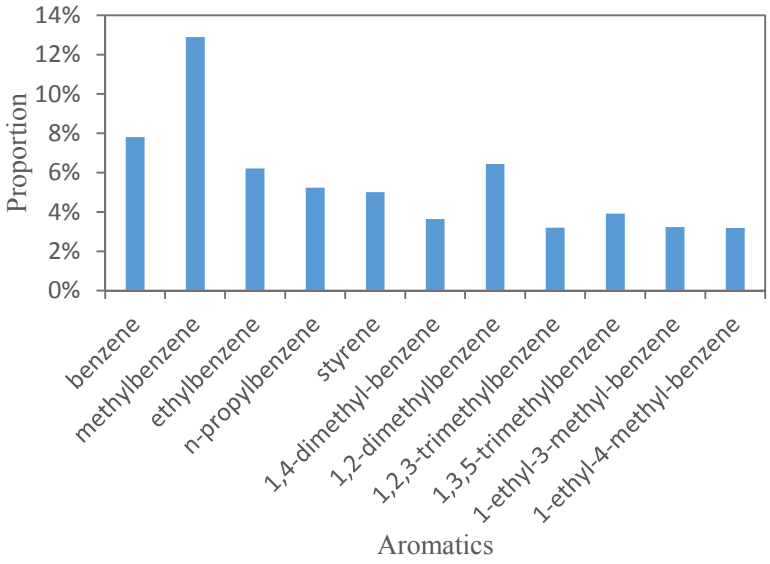

Fig. S6. Composition of aromatics (benzenes) from vehicle exhausts in Longchuan Tunnel.

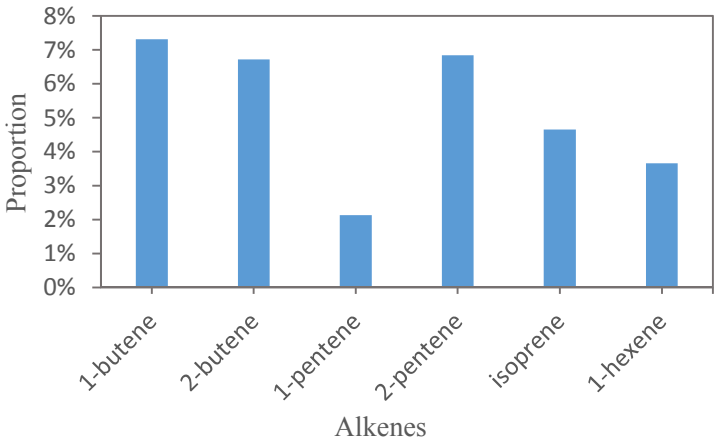

Fig. S7. Composition of alkenes from vehicle exhausts in Longchuan Tunnel.